Supplement of Atmos. Chem. Phys., 22, 5477–5494, 2022
https://doi.org/10.5194/acp-22-5477-2022-supplement

Atmospheric Chemistry and Physics
Open Access
EGU

Supplement of

Global simulations of monoterpene-derived peroxy radical fates and the distributions of highly oxygenated organic molecules (HOMs) and accretion products

Ruochong Xu et al.

Correspondence to: Joel A. Thornton (joelt@uw.edu)

Text S1. Updates to the GEOS-Chem MT Oxidation Mechanism

Table S1. Names and descriptions of new species added in the mechanism.

Name	Description	Molecular weight (g/mol)
MT-bRO2	RO_2 from MT+O_3/OH that can undergo autoxidation	200
MT-cRO2	RO_2 from MT-bRO2 autoxidation	232
MT-HOM-RO2	RO_2 from MT-cRO2 autoxidation	264
aHOM-non-ON	HOM product from HO_2 reaction	278
bHOM-non-ON	HOM product without nitrate from NO and NO_3 reaction	278
HOM-ON	HOM product with nitrate from NO reaction	293
C10-CBYL	Carbonyl with 10 carbon atoms	185
C10-ROH	Alcohol with 10 carbon atoms	185
C20ROOR	Accretion product from C_{10}-RO_2 + C_{10}-RO_2	400
C15ROOR	Accretion product from C_5-RO_2 + C_{10}-RO_2	310
C20DIMER*	Accretion product from HOM-C_{10}-RO_2 + HOM-C_{10}-RO_2	526
C20CROSS*	Accretion product from HOM-C_{10}-RO_2 + C_{10}-RO_2 (except HOM-RO_2)	462
C15CROSS*	Accretion product from HOM-C_{10}-RO_2 + C_5-RO_2	380

*Only appear in the test simulation with a unity branching to accretion products of self- and cross-reactions.

Table S2. Species that initially exist in GEOS-Chem and are used in the newly-added reactions as shown below.

Name	Description
MTPA	Lumped monoterpenes: a-pinene, b-pinene, sabinene, carene
MTPO	Other monoterpenes: Terpinene, terpinolene, myrcene, ocimene, other monoterpenes
RIO2	HOCH2C(OO)(CH3)CH=CH2; RO2 from isoprene, aka ISOPO2
LIMO	Limonene
PIO2	RO_2 from monoterpenes
LIMO2	RO_2 from limonene
KO2	RO_2 from >3 ketones
RCHO	CH3CH2CHO; >= C3 aldehydes
MEK	RC(O)R; Methyl ethyl ketone
ETO2	CH3CH2OO; Ethylperoxy radical
PRPE	C3H6; >= C3 alkenes
MACR	CH2=C(CH3)CHO; Methacrolein
RCOOH	C2H5C(O)OH; > C2 organic acids
HC5	HOCH2CH=C(CH3)CHO; Hydroxycarbonyl with 5C
ROH	C3H7OH; > C2 alcohols

MVK	CH2=CHC(=O)CH3; Methyl vinyl ketone
DIBOO	Dibble peroxy radical
MCO3	CH3C(O)OO; Peroxyacetyl radical
MO2	CH3O2; Methylperoxy radical
MOH	CH3OH; Methanol
ACET	CH3C(O)CH3; Acetone
MONITS	Saturated 1st gen monoterpene organic nitrate
MONIUS	Unsaturated 1st gen monoterpene organic nitrate

Note that in this study, we define MT-aRO2 as RO_2 from monoterpenes and limonene (although limonene is also a kind of monoterpenes, it is a separated species in GEOS-Chem) that initially exist in GEOS-Chem "tropchem" mechanism, namely PIO2 and LIMO2 (See Table S2). Here we use MT-aRO2 for convenience but PIO2 and LIMO2 are still treated separately in the mechanism. Also, MT means monoterpenes (MTPA and MTPO, see Table S2) not including limonene, but when MT is used as a prefix of species name (e.g., MT-bRO2), it represents products from monoterpenes including limonene.

The newly-added species were all set to be "advected", and thus they can undergo transport, convection and PBL-mixing. Some reactions below have already been included in GEOS-Chem but we modified part of them for better representation of RO_2 and HOM chemical fates. The self-/cross-reactions of MT-RO_2, autoxidation and HOM formation are not included in the initial GEOS-Chem mechanism, and we added these into "tropchem" mechanism. We introduce the newly-added species and related reactions in detail below.

(1) Monoterpenes oxidation

(a) OH radical oxidation

For MT/LIMO + OH reaction, we added the MT-bRO2 branching. MT-bRO2 will undergo autoxidation while MT-aRO2 will not. The values of branching ratios $\mathrm{f_{aOH}}$ and $\mathrm{f_{bOH}}$ are shown in Table S3.

$$\mathrm{MT\&LIMO + OH \rightarrow f_{aOH}(MT\text{-}aRO2) + f_{bOH}\,(MT\text{-}bRO2)} \quad (1)$$

(b) Ozonolysis

For MT/LIMO + O_3 reaction, initially no PIO2 or LIMO2 is generated. We added MT-aRO2 and MT-bRO2 branching for the reactions, and modified some products for carbon conservation (although this must be imperfect in the model). Also, new species C10-carbonyl was added as a product here:

$$\begin{aligned}\mathrm{MT + O_3 \rightarrow f_{aO_3}(MT\text{-}aRO2) + f_{bO_3}\,(MT\text{-}bRO2) + 0.85(OH) + 0.2(CO) + 0.02(H2O2)}\\ \mathrm{+ 0.2(C10\text{-}CBYL)} \quad (2)\\ \mathrm{LIMO + O_3 \rightarrow f_{aO_3}(MT\text{-}aRO2) + f_{bO_3}\,(MT\text{-}bRO2) + 0.2(C10\text{-}CBYL) + 0.85(OH) + 0.1(HO2)}\\ \mathrm{+ 0.16(ETO2) + 0.020(H2O2) + 0.14(CO) + 0.46(PRPE) + 0.040(CH2O)}\\ \mathrm{+ 0.29(MACR) + 0.01(HCOOH) + 0.07(RCOOH)} \quad (3)\end{aligned}$$

The values of branching ratios f_{aOH}/f_{bOH} and f_{aO_3}/f_{bO_3} are shown in Table S3 and the range of

choices reflects those values reported in the literature (Ehn et al., 2014; Jokinen et al., 2015; Xu et al., 2019; Zhao et al., 2018). "HighProd" and "LowProd" represent high and low branching fractions of MT-bRO2, respectively.

Table S3. The branching ratios for first generation of MT-RO2 from MT oxidation.

Branching ratio	LowProd	HighProd
f_{aOH}/f_{bOH}	80%:20% (MT) 70%:30% (limonene)	25%:75%
f_{aO_3}/f_{bO_3}	97%:3%	92%:8%

(2) Autoxidation

The H-shift and subsequent autoxidation was added as below:

$$\text{MT-bRO2} \xrightarrow{\text{aut}} \text{MT-cRO2} \xrightarrow{\text{aut}} \text{MT-HOM-RO2} \quad (4)$$

The reaction is temperature-dependent. The barrier energy is referred to Berndt et al (2016). When temperature is 283K, 298K and 310K, corresponding autoxidation rate constants are 0.27 s^{-1}, 1.30 s-1 and 4.12 s-1, respectively. The temperature-dependent rate constants were used in all simulations except experiment LowProd_Photo_kauto_Slow, in which autoxidation rate constant is 1/10 of the values above.

(3) MT-RO2 and ISOP-RO2 self-&cross-reactions

The self- and cross-reactions of isoprene- and MT-derived RO_2 were newly added except the isoprene-derived RO_2 self-reaction that exist initially. It has been demonstrated there are three branches from self- and cross-reactions. The first pathway is to produce an alcohol and an aldehyde. For simplification in this study, a C10-ROH and a C10-CBYL are generated in this pathway. The second pathway is to generate RO radicals, which can further react with O_2 or decompose into smaller compounds. Here we assume that half of RO react with O_2 to produce HO_2 and C_{10}-carbonyl, and the other half decompose into smaller carbonyls. Yet for the self- and cross-reactions involving MT-aRO2 and ISOP-RO2, we also consider another possibility that RO radicals undergo a unimolecular H-shift to form a new RO_2, and thus we have 5% MT-bRO2 formation for these reactions. The third pathway is to produce accretion products (C20ROOR and C15ROOR). The branching ratios of the three pathways above were set as 29%, 67% and 4%, respectively following previous studies (Berndt et al., 2018a, 2018b; Zhao et al., 2018). The reactions are shown in detail below.

(a) When only MT-aRO2 (PIO2&LIMO2) and ISOP-RO2 participate:

$$\begin{aligned}&\text{MT-aRO}_2 + \text{MT-aRO}_2 \\ &\rightarrow \mathrm{f_1}(\text{C10-CBYL} + \text{C10-ROH}) + \mathrm{f_2}[0.45(2\mathrm{HO_2} + 2\text{C10-CBYL}) + 0.5(4\text{HC5}) \\ &+ 0.05(2\text{MT-bRO2})] + \mathrm{f_3}(\text{C20ROOR}) \quad (5)\end{aligned}$$

$$\text{MT-aRO}_2 + \text{ISOP-RO}_2$$
$$\rightarrow f_1[0.5(\text{C10-CBYL}) + 0.5(\text{HC5}) + 0.5(\text{C10-ROH}) + 0.5(\text{ROH})]$$
$$+ f_2[0.45(2\text{HO}_2 + \text{C10-CBYL} + \text{HC5}) + 0.5(3\text{HC5}) + 0.05(\text{MT-bRO2} + \text{HC5}]$$
$$+ f_3(\text{C15ROOR}) \quad (6)$$

(b) When MT-bRO2/MT-cRO2/MT-HOM-RO2 participate:

$$\text{MT-RO}_2 + \text{MT-RO}_2$$
$$\rightarrow f_1(\text{C10-CBYL} + \text{C10-ROH}) + f_2[0.5(2\text{HO}_2 + 2\text{C10-CBYL}) + 0.5(4\text{HC5})]$$
$$+ f_3(\text{C20ROOR}) \quad (7)$$
$$\text{MT-RO}_2 + \text{ISOP-RO}_2$$
$$\rightarrow f_1[0.5(\text{C10-CBYL}) + 0.5(\text{HC5}) + 0.5(\text{C10-ROH}) + 0.5(\text{ROH})]$$
$$+ f_2[0.5(2\text{HO}_2 + \text{C10-CBYL} + \text{HC5}) + 0.5(3\text{HC5})] + f_3(\text{C15ROOR}) \quad (8)$$

Considering the uncertainties of self- and cross-reaction rate constants, we applied slow and fast rate constants collected from laboratory studies for sensitivity test (Table S4). Also, it has been pointed out by some studies that the rate constants are faster for more oxygenated radicals (Berndt et al., 2018a, 2018b; Zhao et al., 2018), and thus the rate constants were set to be faster for MT-cRO2 and MT-HOM-RO2 that are generated by autoxidation in this study (shown as $MT(O_2)_nRO2$ in Table S4). We used "Fast" values in all simulations except LowProd_Photo_Slow, in which self- and cross-reactions rate constants are "Slow" values.

Table S4. Rate constants for self- and cross-reactions of isoprene- and MT-derived RO_2.

	Slow	Fast
MT-RO2 + MT-RO2	1.0×10^{-12} [a]	4.0×10^{-11} [b]
$MT(O_2)_nRO2$ + $MT(O_2)_nRO2$	4.0×10^{-11} [b]	2.6×10^{-10} [c]
MT-RO2 + $MT(O_2)_nRO2$	1.0×10^{-12} [a]	2.6×10^{-10} [c]
MT-RO2 + ISOP-RO2	2.0×10^{-11} [b]	
$MT(O_2)_nRO2$ + ISOP-RO2	4.0×10^{-11} [d]	
ISOP-RO2 + ISOP-RO2	Default in GEOS-Chem	

(4) MT-RO2 reactions with methylperoxy/peroxyacetyl radicals

The reactions between MT-RO2 (PIO2 and LIMO2) and methylperoxy (MO2)/peroxyacetyl radicals (MCO3) exist initially in GEOS-Chem mechanism. We modified parts of the reactions especially the products for better representation as shown below. The rate constants remain unchanged following initial values in GEOS-Chem.

(a) When only MT-aRO2 (PIO2&LIMO2) participate:

$$\text{PIO2} + \text{MO2} = 0.3[0.5\text{CH2O} + 0.5\text{MOH} + 0.5\text{C10-ROH} + 0.5\text{C10-CBYL}]$$
$$+ 0.65[2\text{HO2} + \text{CH2O} + \text{HC5} + \text{RCHO} + \text{RCOOH}]$$
$$+ 0.05[\text{HO2} + \text{CH2O} + \text{MT-}\beta\text{RO2}] \quad (9)$$
$$\text{PIO2} + \text{MCO3} = 0.7[\text{MO2} + \text{HO2} + \text{HC5} + \text{RCHO} + \text{RCOOH}]$$
$$+ 0.25[\text{ACTA} + 0.5\text{C10-ROH} + 0.5\text{C10-CBYL}]$$
$$+ 0.05[\text{MO2} + \beta\text{MTRO2}] \quad (10)$$

$$\mathrm{LIMO2} + \mathrm{MO2} = 0.7[\mathrm{HO2} + \mathrm{CH2O} + 0.5\mathrm{PRPE} + 0.5\mathrm{MACR} + 0.5\mathrm{HC5}] + 0.25[0.5\mathrm{C10\text{-}CBYL} + 0.5\mathrm{C10\text{-}ROH} + 0.5\mathrm{MOH} + 0.5\mathrm{CH2O}] + 0.05[\mathrm{MT\text{-}\beta RO2} + \mathrm{HO2} + \mathrm{CH2O}] \quad (11)$$

$$\mathrm{LIMO2} + \mathrm{MCO3} = 0.7[\mathrm{MO2} + \mathrm{HO2} + 0.5(\mathrm{PRPE} + \mathrm{MACR}) + \mathrm{HC5}] + 0.25[\mathrm{ACTA} + 0.5\mathrm{C10\text{-}ROH} + 0.5\mathrm{C10\text{-}CBYL}] + 0.05[\mathrm{MO2} + \mathrm{MT\text{-}\beta RO2}] \quad (12)$$

(b) When MT-bRO2/MT-cRO2/MT-HOM-RO2 participate:

$$\mathrm{MT\text{-}RO2} + \mathrm{MO2} = 0.3[0.5\mathrm{CH2O} + 0.5\mathrm{MOH} + 0.5\mathrm{C10\text{-}ROH} + 0.5\mathrm{C10\text{-}CBYL}] + 0.7[2\mathrm{HO2} + \mathrm{CH2O} + \mathrm{HC5} + \mathrm{RCHO} + \mathrm{RCOOH}] \quad (13)$$

$$\mathrm{MT\text{-}RO2} + \mathrm{MCO3} = 0.7[\mathrm{MO2} + \mathrm{HO2} + \mathrm{HC5} + \mathrm{RCHO} + \mathrm{RCOOH}] + 0.3[\mathrm{ACTA} + 0.5\mathrm{C10\text{-}ROH} + 0.5\mathrm{C10\text{-}CBYL}] \quad (14)$$

(5) MT-RO2 reactions with NO/NO_3

(a) NO reaction

To preserve as much as possible the current simplified framework for MT chemistry in GEOS-Chem, all new MT-RO2 species are allowed to react with NO following the initial MT-RO2+NO reaction in GEOS-Chem. Yet for MT-aRO2, a 5% branching of MT-bRO2 formation was added. This is because in polluted regions, the formation of HOM may well be facilitated by certain NO reactions through the alkoxy channel.

$$\mathrm{PIO2} + \mathrm{NO} = 0.820\mathrm{HO2} + 0.820\mathrm{NO2} + 0.230\mathrm{CH2O} + 0.380\mathrm{RCHO} + 0.110\mathrm{ACET} + 0.440\mathrm{MEK} + 0.070\mathrm{HCOOH} + 0.120\mathrm{MONITS} + 0.060\mathrm{MONITU} + 0.05\mathrm{MT\text{-}bRO2} \quad (15)$$

$$\mathrm{LIMO2} + \mathrm{NO} = 0.686\mathrm{HO2} + 0.780\mathrm{NO2} + 0.220\mathrm{MONITU} + 0.289\mathrm{PRPE} + 0.231\mathrm{CH2O} + 0.441\mathrm{RCHO} + 0.058\mathrm{HAC} + 0.289\mathrm{MEK} + 0.05\mathrm{MT\text{-}bRO2} \quad (16)$$

(b) NO_3 reaction

We modified the initial MT-aRO2+NO3 reactions in GEOS-Chem to include the new species C10-CBYL as product and a 5% branch of MT-bRO2 formation.

$$\mathrm{PIO2} + \mathrm{NO3} = \mathrm{HO2} + \mathrm{NO2} + 0.25\mathrm{C10\text{-}CBYL} + 0.7(\mathrm{HC5} + \mathrm{RCOH}) + 0.05\mathrm{MT\text{-}bRO2} \quad (17)$$

$$\mathrm{LIMO2} + \mathrm{NO3} = \mathrm{HO2} + \mathrm{NO2} + 0.25\mathrm{C10\text{-}CBYL} + 0.7\big(0.7(\mathrm{HC5} + \mathrm{RCHO}) + 0.3(\mathrm{PRPE} + \mathrm{CH2O} + \mathrm{MACR})\big) + 0.05\mathrm{MT\text{-}bRO2} \quad (18)$$

For MT-bRO2, the 5% branching was removed:

$$\mathrm{MT\text{-}bRO2} + \mathrm{NO3} = \mathrm{HO2} + \mathrm{NO2} + 0.3\mathrm{C10\text{-}CBYL} + 0.7(\mathrm{HC5} + \mathrm{ROH}) \quad (19)$$

For MT-cRO2:

$$\mathrm{MT\text{-}cRO_2} + \mathrm{NO_3} = \mathrm{HO_2} + \mathrm{NO_2} + 0.75(\mathrm{C10\text{-}CBYL}) + 0.25(\mathrm{MT\text{-}HOM\text{-}RO_2}) \quad (20)$$

(6) HOM formation and loss pathways

(a) HOM formation

HOM is formed through MT-HOM-RO2 reactions with HO_2/NO/NO_3. Considering radical fragmentation, some carbonyl fragments were added as products in the reactions with NO and NO_3. Three kinds of HOM are formed: aHOM-non-ON and bHOM-non-ON without nitrate and HOM-ON with nitrate. The rate constants are the same as MT-RO2 + HO2/NO/NO_3 reactions in GEOS-Chem.

$$\text{MT-HOM-RO}_2 + \text{HO}_2 = \text{aHOM-non-ON} + \text{O}_2 \quad (21)$$

$$\text{MT-HOM-RO}_2 + \text{NO} = 0.8\text{NO}_2 + 0.8\text{HO}_2 + 0.8(0.5\text{bHOM-non-ON} + \text{HC5}) + 0.2\text{HOM-ON} \quad (22)$$

$$\text{MT-HOM-RO}_2 + \text{NO}_3 = \text{HO}_2 + \text{NO}_2 + 0.5\text{bHOM-non-ON} + \text{HC5} \quad (23)$$

(b) Photolysis

Photolysis is allowed for all HOM species with the same rate constant. The value of the photolysis frequency is based on how well the model reproduces HOM observations in the absence of further photochemical degradation, and also on laboratory chamber experiments showing loss of HOM and MTSOA mass over time (Pospisilova et al., 2020; Zawadowicz et al., 2020). It is set as about 1/60 of NO_2 photolysis rate in GEOS-Chem.

(c) Deposition

We parameterize HOM wet deposition following the same parameters of aerosol-phase organic nitrate in Fisher et al. (2016), and dry deposition is calculated online based on the resistance-in-series algorithm (Zhang et al., 2001). The parameters used are shown in Table S5.

Table S5. Parameters used in HOM deposition parameterization.

Parameters	Description	Value
DD_DvzAerSnow	DD_DvzAerSnow specifies the dry deposition velocity over ice and snow. This usually 0.03 cm/s.	0.03
WD_AerScavEff	Specifies the aerosol scavenging efficiency. This factor is used to calculate loss by convective updraft scavenging	0.8
WD_KcScaleFac	Specifies a temperature-dependent scale factor that is used to calculate conversion of cloud condensate to precipitation	1.0 (0.5 when 237 K <= temperature < 258 K)
WD_RainoutEff	Specifies a temperature-dependent scale factor that is used to calculate scavenging by rainout	0.8 (0 when 237 K <= temperature < 258 K)

(7) C10 carbonyl and alcohol

(a) Formation

New species C10 carbonyl and alcohol are formed from the related reactions shown above.

(b) Chemical Loss

The only reaction pathway of new species C10-CBYL and C10-ROH is reaction with OH radical now. The rate constant is the same as ROH+OH in GEOS-Chem.

$$\text{C10-CBYL} + \text{OH} \rightarrow 0.50(\text{MT-aRO}_2) + 0.475(\text{MT-bRO}_2) + 0.025(\text{MT-cRO2}) \quad (24)$$

$$\text{C10-ROH} + \text{OH} \rightarrow 0.50(\text{MT-aRO}_2) + 0.475(\text{MT-bRO}_2) + 0.025(\text{MT-cRO2}) \quad (25)$$

(c) Deposition

The C10-CBYL and C10-ROH are dry- and wet-deposited using the same parameters as acetic acid in GEOS-Chem.

(8) Accretion products

The accretion products C20ROOR and C15ROOR do not have chemical loss yet, so the mass concentrations are likely to be a high-limit estimate. The only loss pathway of accretion products is dry and wet deposition. Considering their expected low volatility, they are dry- and wet-deposited using the same parameters as HOM species as shown in Table S5.

Text S2. Observation Data

(1) SENEX, the United States (2013)

The SENEX (Southeast Nexus) campaign was carried out in southeast U.S. in summer 2013 for studying the interactions between natural and anthropogenic emissions at the nexus of climate change and air quality (Carlton et al., 2018). The details of the campaign and measurement datasets were available online (https://www.esrl.noaa.gov/csl/projects/senex/). In this study, the data at Centreville site, Alabama was used for comparison with the simulation results.

Measurement data of organic nitrate (ON) was from June 4 to July 16, 2013. The instrument used was HR-ToF-CIMS with iodide-adduct ionization high-resolution time-of-flight mass spectrometry. Both gas- and particle-phase ON were measured and the molecular formulas of top 5 contributing gas- and particle-phase species are shown in Table S6. The organic aerosol mass concentrations were measured using HR-ToF-AMS.

Table S6. Molecular formulas of top 5 contributing HOM-ON and HOM-non-ON species (gas- and particle-phase) at Centreville, Alabama

HOM-ON		**HOM-non-ON**	
Gas-phase	**Particle-phase**	**Gas-phase**	**Particle-phase**
C10H15O7N1	C10H15O7N1	C10H14O7	C10H14O7
C10H17O7N1	C10H15O8N1	C10H12O7	C10H12O7
C10H15O8N1	C10H17O7N1	C10H22O8	C10H16O7
C10H17O8N1	C10H17O8N1	C10H22O7	C10H22O8
C10H13O8N1	C10H15O9N1	C10H16O7	C10H22O7

(2) BAECC, Finland (2014)

The field study on Biogenic Aerosols-Effects on Clouds and Climate (BAECC 2014) was conducted at the Station for Measuring Ecosystem Atmosphere Relations (SMEAR II) in Hyytiälä

Finland (Petaja et al., 2016). The SMEAR II site is situated in a remote, monoterpene-dominated pine forest. More details are available online (http://www.actris.net/language/en-GB/TransNationalAccess/Callforproposals/WP10SpecificcallforTNA2014.aspx).

Measurement data of HR-ToF-CIMS was from April 11 to June 3, 2014 based on iodide-adduct ionization high-resolution time-of-flight mass spectrometry. Both gas- and particle-phase organic compounds were measured and the molecular formulas of top 5 contributing gas- and particle-phase species are shown in Table S7.

Table S7. Molecular formulas of top 5 contributing HOM-ON and HOM-non-ON species (gas- and particle-phase) at Hyytiälä, Finland

HOM-ON		**HOM-non-ON**	
Gas-phase	**Particle-phase**	**Gas-phase**	**Particle-phase**
C10H15O7N1	C10H15O8N1	C10H12O11	C10H14O7
C10H15O8N1	C10H15O7N1	C10H14O8	C10H22O9
C10H17O7N1	C10H17O7N1	C10H16O8	C10H22O7
C10H13O7N1	C10H17O8N1	C10H14O7	C10H22O8
C10H17O8N1	C10H15O9N1	C10H22O7	C10H16O7

(3) GoAmazon, Brazil (2014)

The Green Ocean Amazon Experiment (GoAmazon) aimed to observe pollution affecting gases, aerosols, clouds, and rainfall over the Amazon rain forest (Martin et al., 2016). It lasted from 2014-2015 covering both wet and dry seasons, but merely wet-season data (February 6 to March 29, 2014) was used in this study because of the dominating impact of biomass burning in dry season that can bias comparison with biogenic-source species.

No CIMS-measured HOM data was available during the campaign, so we only used organic aerosol mass concentrations from AMS instrument.

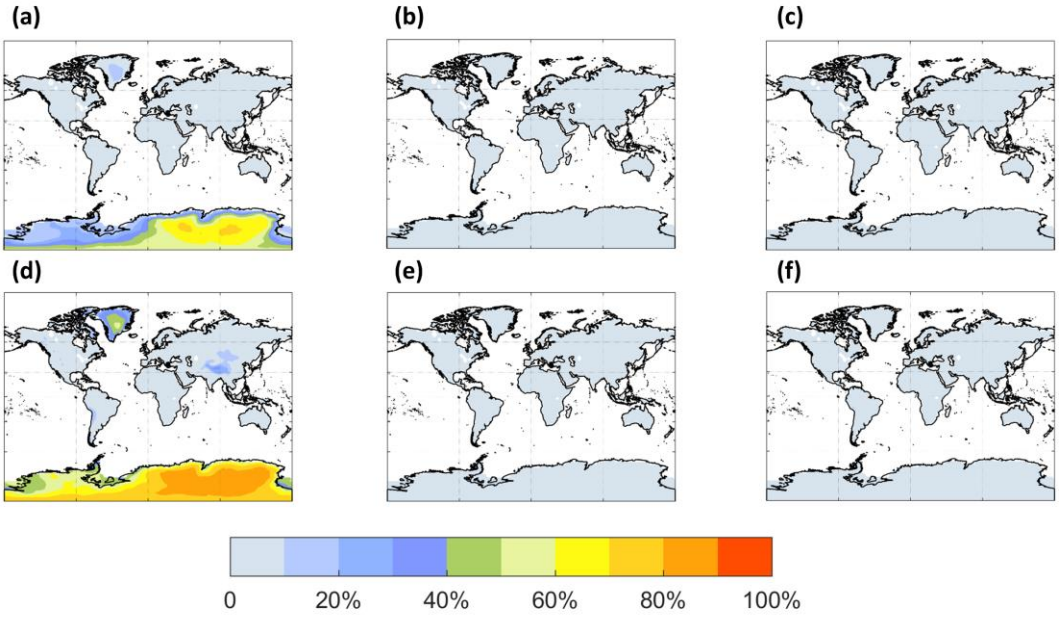

Figure S1. The annually PBL-averaged MT-bRO2 consumption fractions by HO_2 (left panel), NO_3 (middle panel) and RO_2 (right panel) from experiments LowProd_Photo (a)-(b) and LowProd_Photo_kauto_Slow (c)-(d). Autoxidation rate constant is ~1.0 s-1 and ~0.1 s-1 at 298K in two experiments, respectively.

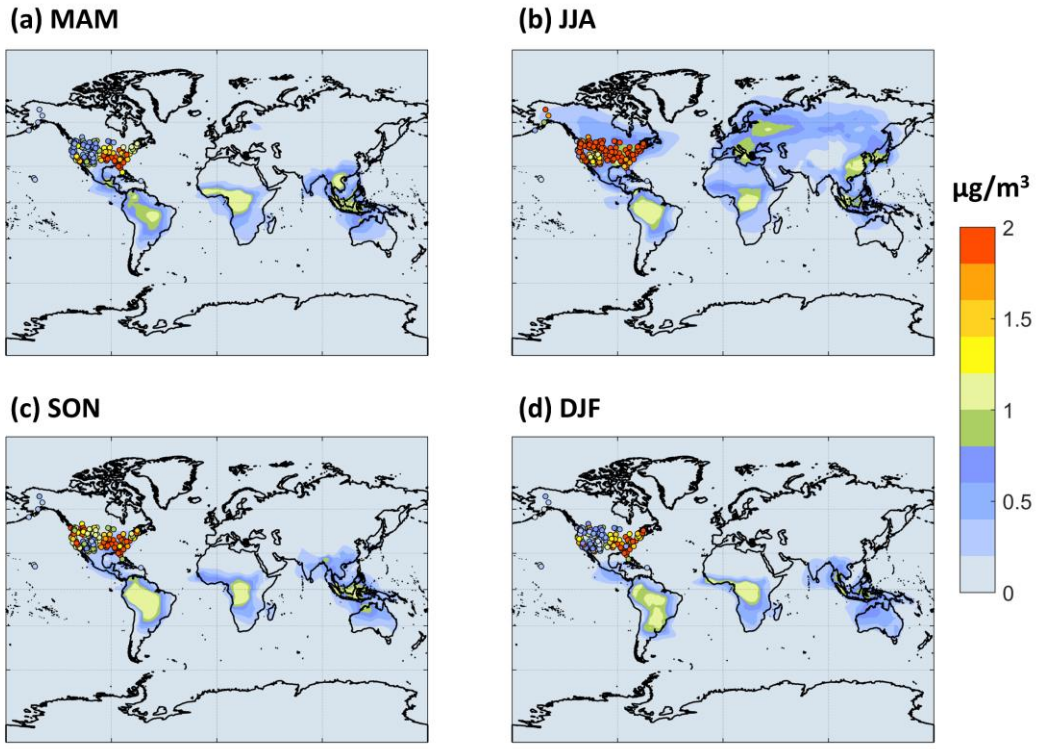

Figure S2. The same as Figure 7 (a)-(d). The seasonal organic aerosol mass concentrations from IMPROVE sites are also presented. The unit is µg/m^3.

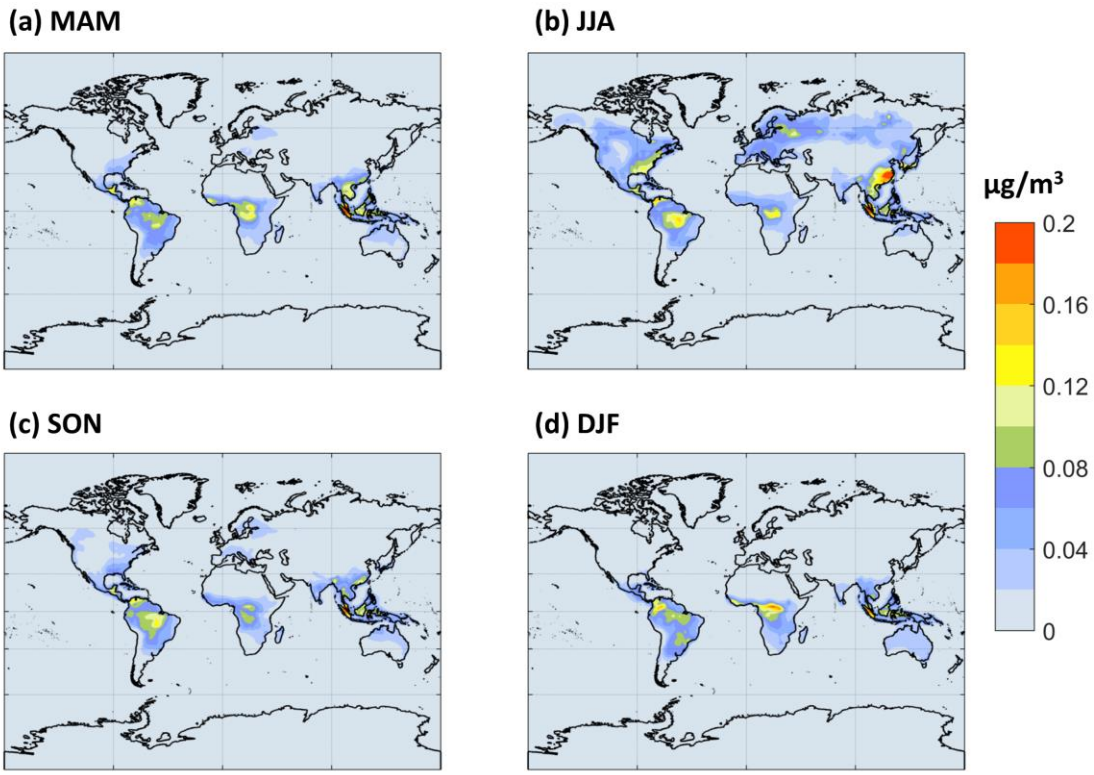

Figure S3. The same as Fig.7 but the results are from experiment LowProd_Photo.

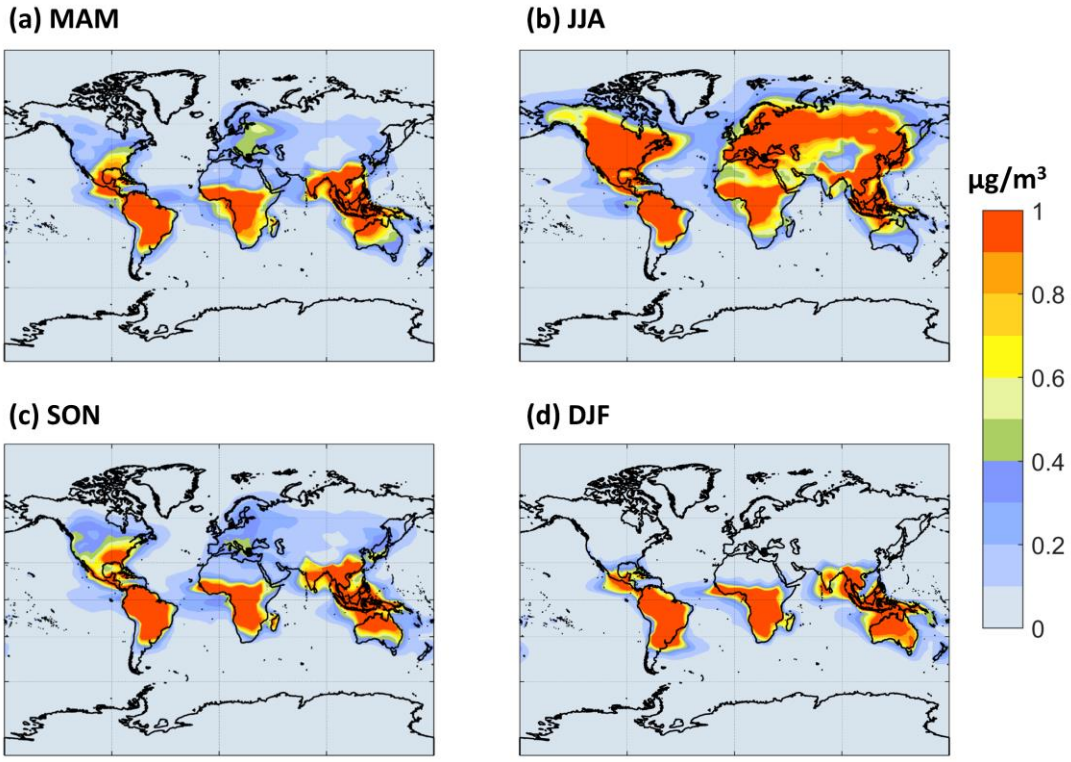

Figure S4. The same as Fig.7 but the results are from experiment HighProd_noPhoto.

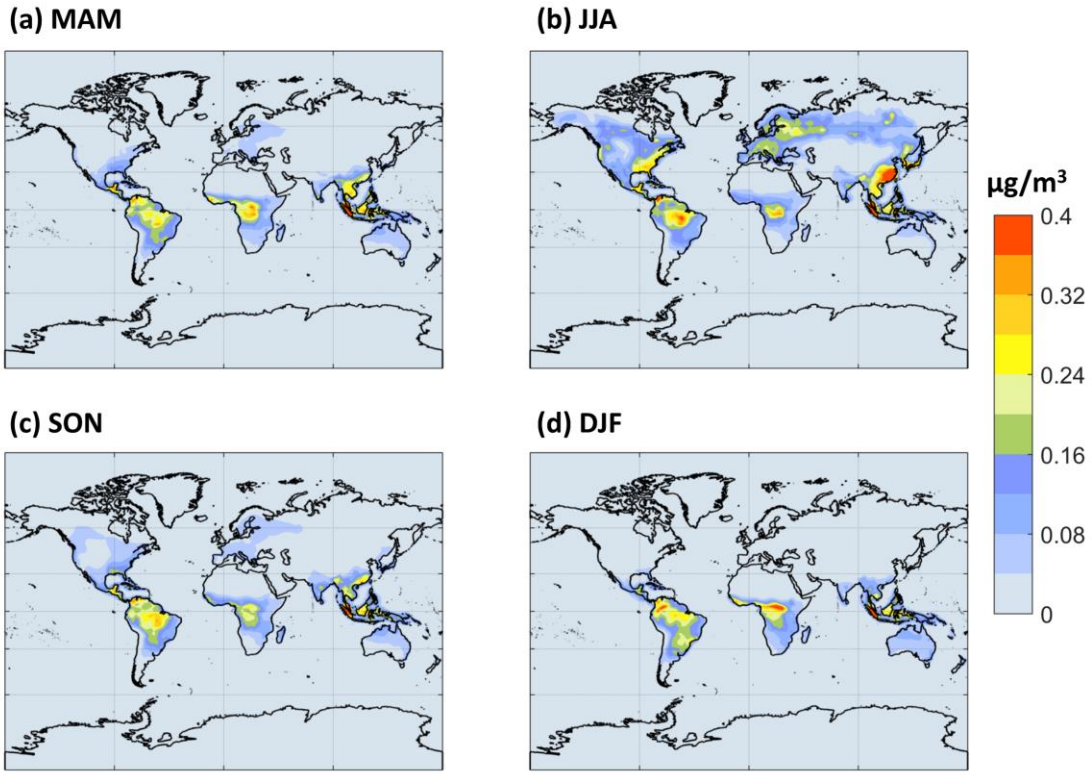

Figure S5. The same as Fig.7 but the results are from experiment HighProd_Photo.

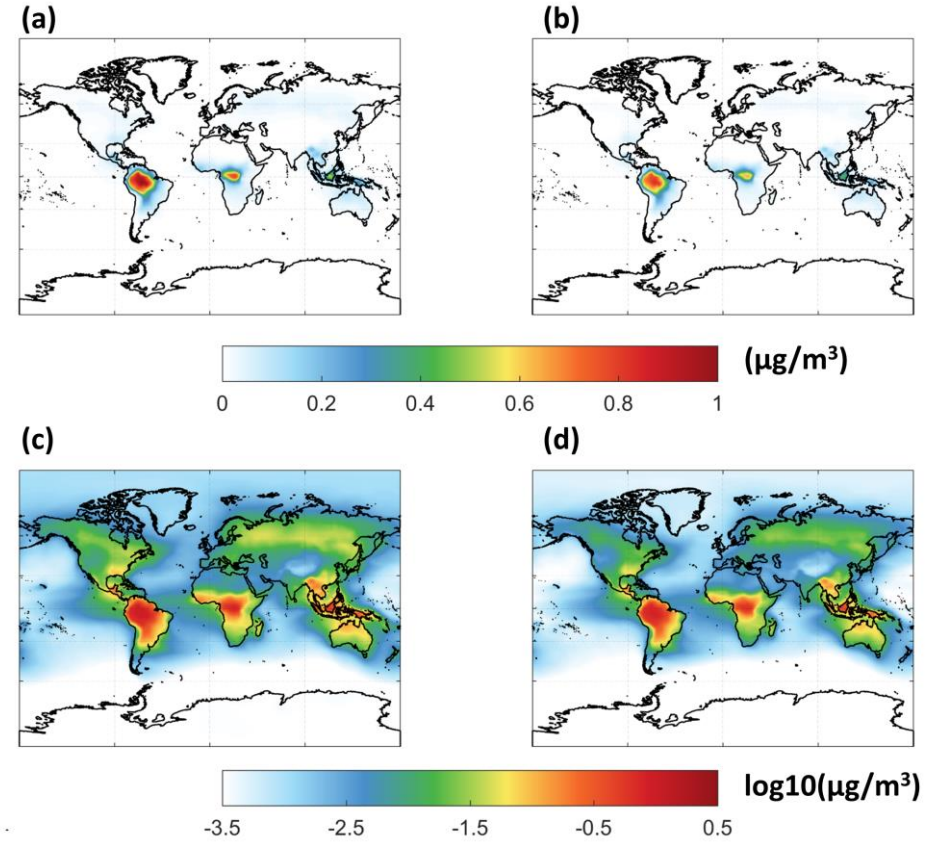

Figure S7. The annually PBL-averaged total accretion product (C20 and C15) mass concentrations from simulation (a) LowProd_Photo and (b) LowProd_Photo_Slow, where

accretion products are assumed to form at 4% branching per MT-RO_2 self and cross reactions. (c)-(d) The same as (a)-(b) but in $\log_{10}$-scale.

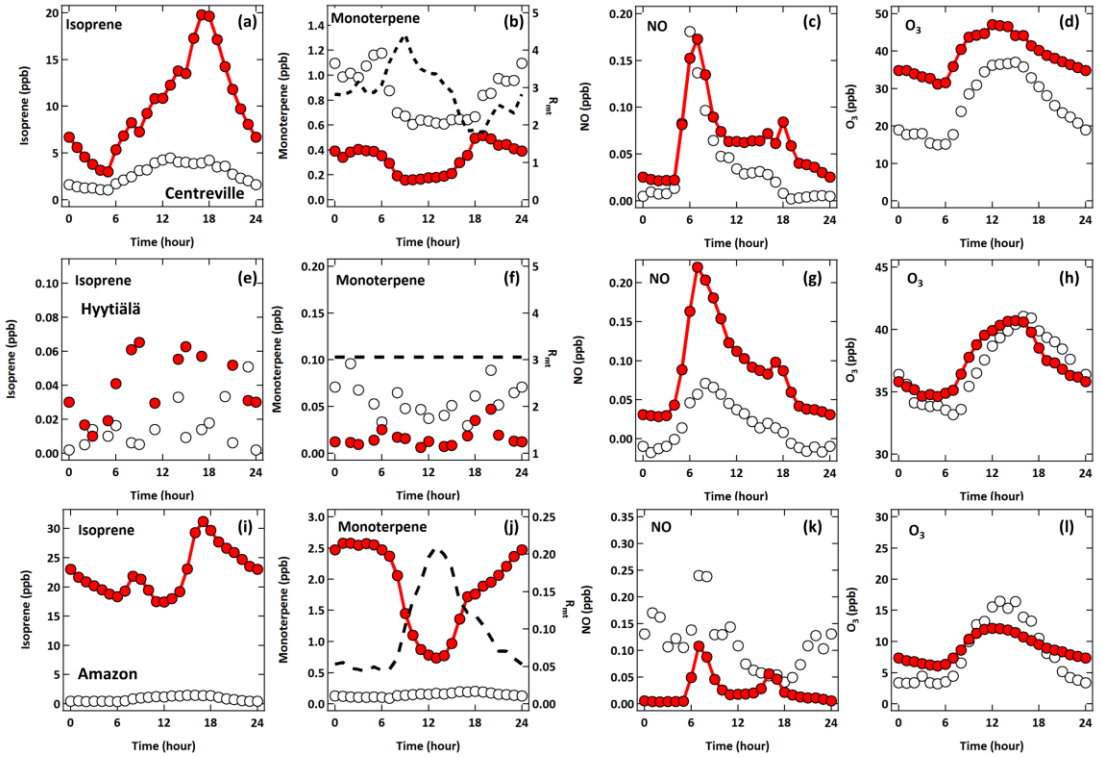

Figure S8. (a)-(d) Diurnal cycles of observed (white circle markers) and simulated (red line) concentrations of isoprene, monoterpenes, NO and O_3 at Centerville site, Alabama. Simulated concentrations are taken from the lowest vertical level of the model, with a centroid altitude typically about 60 m above ground level. The dashed black line in the subplot of monoterpenes represents the diurnal cycle of the ratios of observed to simulated monoterpene concentrations. (e)-(h) The same as (a)-(d) but at Hyytiälä site, Finland. (i)-(l) The same as (a)-(d) but at GoAmazon T3 site, Brazil. For Centreville and GoAmazon T3 sites, hourly average measured monoterpene data was used to compare with the hourly GEOS-Chem simulation and obtain the ratios as shown in (b) and (j), while for the Hyytiälä site, the average measured monoterpene concentrations during the campaign were used, and thus the ratio diurnal cycle is unchanged as shown in (f).

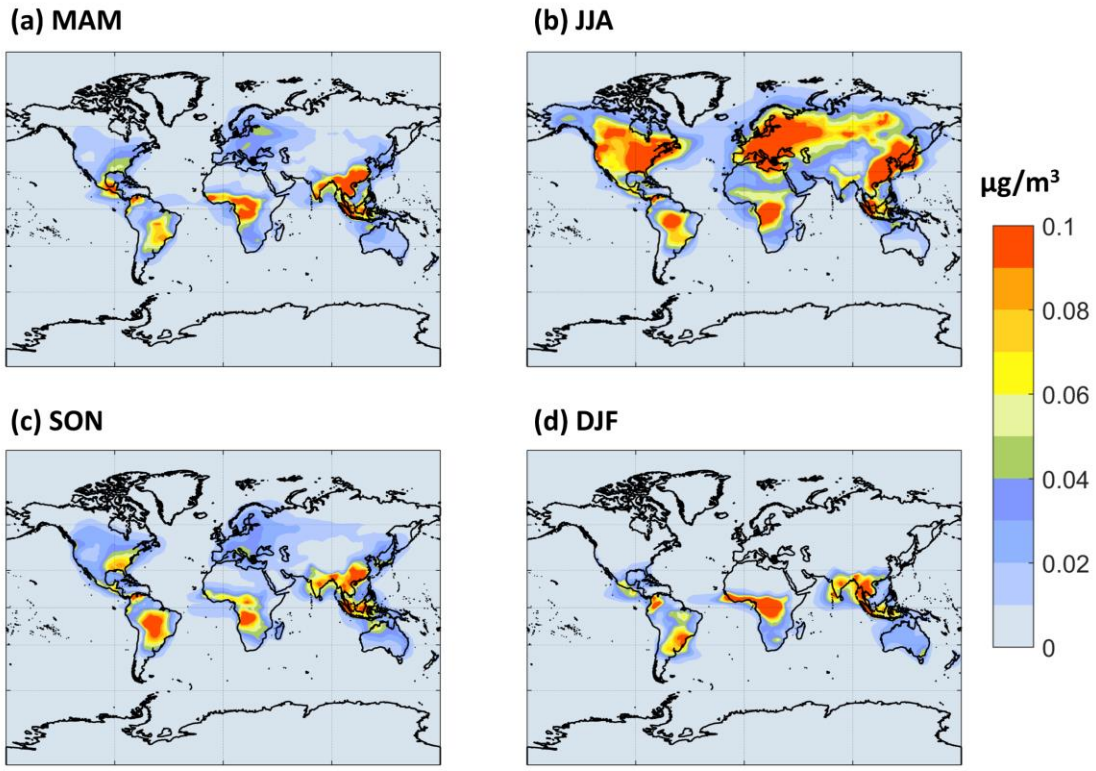

Figure S9. The same as for Fig.7 but here only concentrations of HOM-ON are shown.

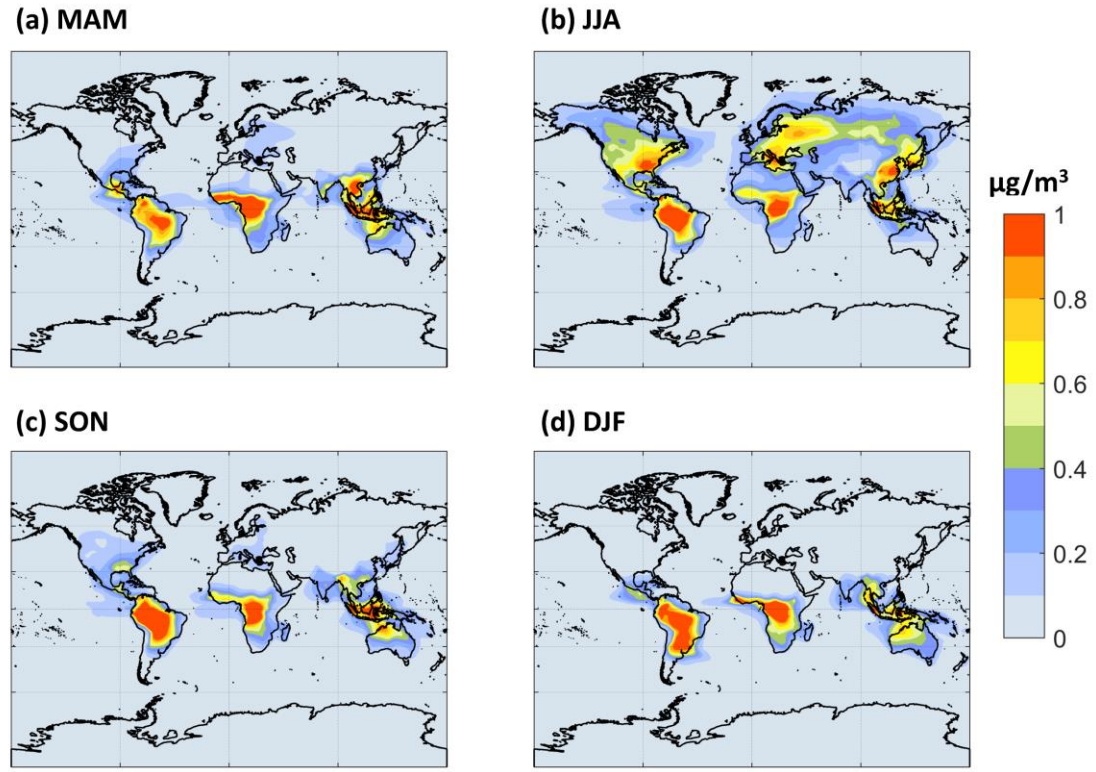

Figure S10. The same as Fig.7 but here only concentrations of HOM-non-ON are shown.

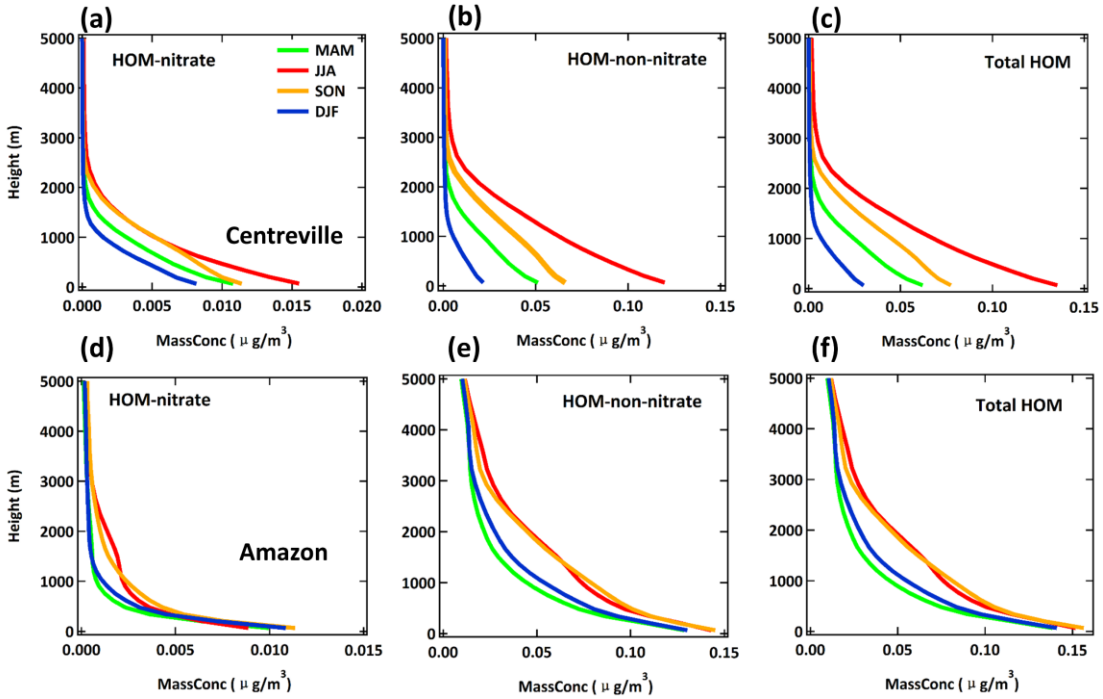

Figure S11. The seasonal averaged vertical profiles of HOM-ON (left panel), HOM-non-ON (middle panel) and total HOM (right panel) at Centreville (top panel) and Amazon (bottom panel).

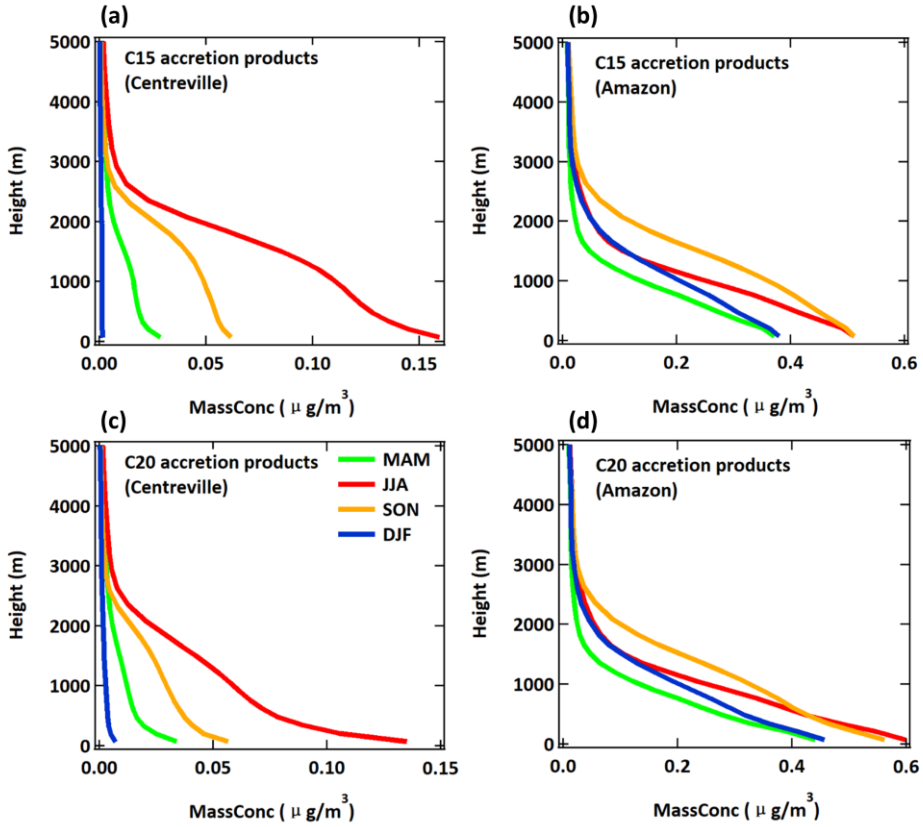

Figure S12. The seasonal averaged vertical profiles of C_{15} accretion products at (a) Centreville and (b) Amazon from experiment LowProd_Photo (default assumption: 4% branching of accretion products from cross- and self-reactions). (c)-(d) The same as (a)-(b) but for C_{20} accretion products.

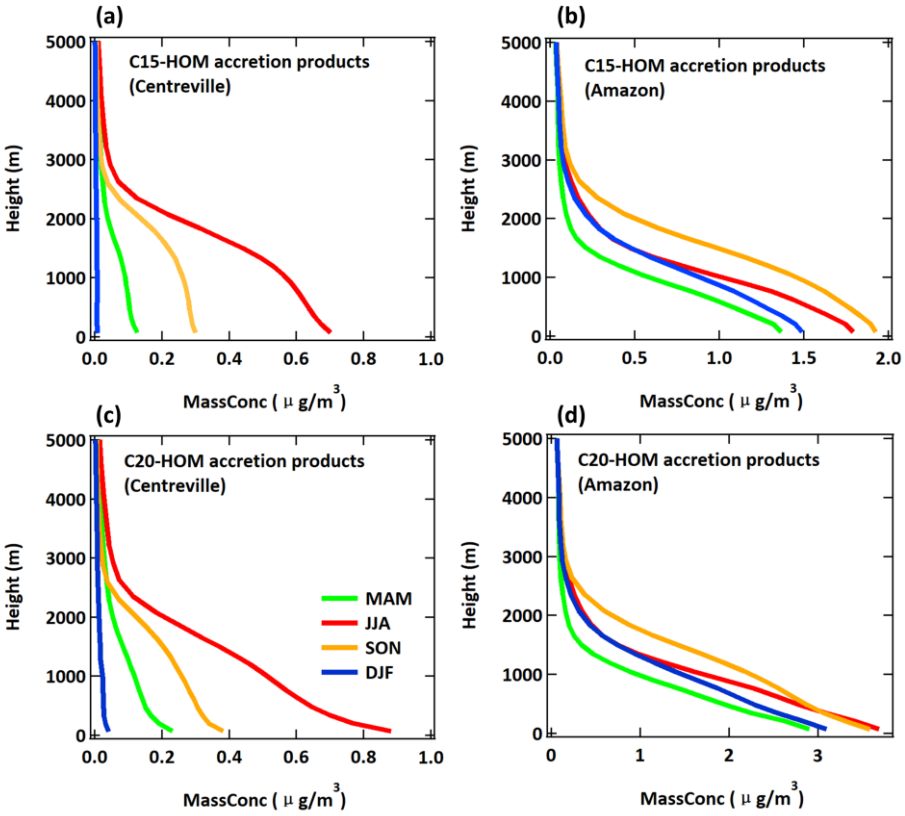

Figure S13. The seasonal averaged vertical profiles of C_{15} HOM accretion products at (a) Centreville and (b) Amazon from experiment LowProd_Photo with branching ratio of unity for HOM-RO_2 derived accretion products. (c)-(d) The same as (a)-(b) but for C_{20} HOM accretion products.

References

Berndt, T., Richters, S., Jokinen, T., Hyttinen, N., Kurtén, T., Otkjær, R. V., Kjaergaard, H. G., Stratmann, F., Herrmann, H., Sipilä, M., Kulmala, M. and Ehn, M.: Hydroxyl radical-induced formation of highly oxidized organic compounds, Nat. Commun., 7(May), 13677, doi:10.1038/ncomms13677, 2016.

Berndt, T., Mentler, B., Scholz, W., Fischer, L., Herrmann, H., Kulmala, M. and Hansel, A.: Accretion Product Formation from Ozonolysis and OH Radical Reaction of α-Pinene: Mechanistic Insight and the Influence of Isoprene and Ethylene, Environ. Sci. Technol., doi:10.1021/acs.est.8b02210, 2018a.

Berndt, T., Scholz, W., Mentler, B., Fischer, L., Herrmann, H., Kulmala, M. and Hansel, A.: Accretion Product Formation from Self- and Cross-Reactions of RO2 Radicals in the Atmosphere, Angew. Chemie Int. Ed., 57(14), 3820–3824, doi:https://doi.org/10.1002/anie.201710989, 2018b.

Carlton, A. G., de Gouw, J., Jimenez, J. L., Ambrose, J. L., Attwood, A. R., Brown, S., Baker, K. R., Brock, C., Cohen, R. C., Edgerton, S., Farkas, C. M., Farmer, D., Goldstein, A. H., Gratz, L., Guenther, A., Hunt, S., Jaeglé, L., Jaffe, D. A., Mak, J., McClure, C., Nenes, A., Nguyen, T. K.,

Pierce, J. R., de Sa, S., Selin, N. E., Shah, V., Shaw, S., Shepson, P. B., Song, S., Stutz, J., Surratt, J. D., Turpin, B. J., Warneke, C., Washenfelder, R. A., Wennberg, P. O. and Zhou, X.: Synthesis of the Southeast Atmosphere Studies: Investigating Fundamental Atmospheric Chemistry Questions, Bull. Am. Meteorol. Soc., 99(3), 547–567, doi:10.1175/BAMS-D-16-0048.1, 2018.

Ehn, M., Thornton, J. A., Kleist, E., Sipila, M., Junninen, H., Pullinen, I., Springer, M., Rubach, F., Tillmann, R., Lee, B., Lopez-Hilfiker, F., Andres, S., Acir, I.-H., Rissanen, M., Jokinen, T., Schobesberger, S., Kangasluoma, J., Kontkanen, J., Nieminen, T., Kurten, T., Nielsen, L. B., Jorgensen, S., Kjaergaard, H. G., Canagaratna, M., Dal Maso, M., Berndt, T., Petaja, T., Wahner, A., Kerminen, V.-M., Kulmala, M., Worsnop, D. R., Wildt, J. J., Mentel, T. F., Maso, M. D., Berndt, T., Petaja, T., Wahner, A., Kerminen, V.-M., Kulmala, M., Worsnop, D. R., Wildt, J. J. and Mentel, T. F.: A large source of low-volatility secondary organic aerosol, Nature, 506(7489), 476–479, doi:10.1038/nature13032, 2014.

Fisher, J. A., Jacob, D. J., Travis, K. R., Kim, P. S., Marais, E. A., Chan Miller, C., Yu, K., Zhu, L., Yantosca, R. M., Sulprizio, M. P., Mao, J., Wennberg, P. O., Crounse, J. D., Teng, A. P., Nguyen, T. B., St. Clair, J. M., Cohen, R. C., Romer, P., Nault, B. A., Wooldridge, P. J., Jimenez, J. L., Campuzano-Jost, P., Day, D. A., Hu, W., Shepson, P. B., Xiong, F., Blake, D. R., Goldstein, A. H., Misztal, P. K., Hanisco, T. F., Wolfe, G. M., Ryerson, T. B., Wisthaler, A. and Mikoviny, T.: Organic nitrate chemistry and its implications for nitrogen budgets in an isoprene- and monoterpene-rich atmosphere: constraints from aircraft (SEAC^{4}RS) and ground-based (SOAS) observations in the Southeast US, Atmos. Chem. Phys., 16(9), 5969–5991, doi:10.5194/acp-16-5969-2016, 2016.

Jokinen, T., Berndt, T., Makkonen, R., Kerminen, V.-M., Junninen, H., Paasonen, P., Stratmann, F., Herrmann, H., Guenther, A. B., Worsnop, D. R., Kulmala, M., Ehn, M. and Sipilä, M.: Production of extremely low volatile organic compounds from biogenic emissions: Measured yields and atmospheric implications., Proc. Natl. Acad. Sci. U. S. A., 112(23), 7123–8, doi:10.1073/pnas.1423977112, 2015.

Martin, S. T., Artaxo, P., Machado, L. A. T., Manzi, A. O., Souza, R. A. F., Schumacher, C., Wang, J., Andreae, M. O., Barbosa, H. M. J., Fan, J., Fisch, G., Goldstein, A. H., Guenther, A., Jimenez, J. L., Pöschl, U., Silva Dias, M. A., Smith, J. N. and Wendisch, M.: Introduction: Observations and Modeling of the Green Ocean Amazon (GoAmazon2014/5), Atmos. Chem. Phys., 16(8), 4785–4797, doi:10.5194/acp-16-4785-2016, 2016.

Petaja, T., O'Connor, E. J., Moisseev, D., Sinclair, V. A. V. A., Manninen, A. J. A. J., Vaananen, R., von Lerber, A., Thorntoton, J. A., Nicocoll, K., Petersen, W., Chandrasekar, V., Smith, J. N., Winkler, P. M., Krueger, O., Hakola, H., Timonen, H., Brus, D., Laurila, T., Asmi, E., Riekkola, M.-L., Mona, L., Massoli, P., Engelmann, R., Kompppula, M., Wang, J., Kuang, C., Baeck, J., Virtanen, A., Levula, J., Ritsche, M., Hickmon, N., Petäjä, T., O'Connor, E. J., Moisseev, D., Sinclair, V. A. V. A., Manninen, A. J. A. J., Väänänen, R., von Lerber, A., Thornton, J. A., Nicoll, K., Petersen, W., Chandrasekar, V., Smith, J. N., Winkler, P. M., Krüger, O., Hakola, H., Timonen, H., Brus, D., Laurila, T., Asmi, E., Riekkola, M.-L., Mona, L., Massoli, P., Engelmann, R., Komppula, M., Wang, J., Kuang, C., Bäck, J., Virtanen, A., Levula, J., Ritsche, M. and Hickmon, N.: BAECC: A Field Campaign to Elucidate the Impact of Biogenic Aerosols on Clouds and Climate, Bull. Am. Meteorol. Soc., 97(10), 1909–1928, doi:10.1175/BAMS-D-14-00199.1, 2016.

Pospisilova, V., Lopez-Hilfiker, F. D., Bell, D. M., El Haddad, I., Mohr, C., Huang, W., Heikkinen, L., Xiao, M., Dommen, J., Prevot, A. S. H., Baltensperger, U. and Slowik, J. G.: On the fate of oxygenated organic molecules in atmospheric aerosol particles, Sci. Adv., 6(11), doi:10.1126/sciadv.aax8922, 2020.

Xu, L., Møller, K. H., Crounse, J. D., Otkjær, R. V., Kjaergaard, H. G. and Wennberg, P. O.: Unimolecular reactions of peroxy radicals formed in the oxidation of α-Pinene and β-Pinene by hydroxyl radicals, J. Phys. Chem. A, doi:10.1021/acs.jpca.8b11726, 2019.

Zawadowicz, M. A., Lee, B. H., Shrivastava, M., Zelenyuk, A., Zaveri, R. A., Flynn, C., Thornton, J. A. and Shilling, J. E.: Photolysis Controls Atmospheric Budgets of Biogenic Secondary Organic Aerosol, Environ. Sci. \& Technol., 54(7), 3861–3870, doi:10.1021/acs.est.9b07051, 2020.

Zhang, L., Gong, S., Padro, J. and Barrie, L.: A size-segregated particle dry deposition scheme for an atmospheric aerosol module, Atmos. Environ., 35(3), 549–560, doi:https://doi.org/10.1016/S1352-2310(00)00326-5, 2001.

Zhao, Y., Thornton, J. A. and Pye, H. O. T.: Quantitative constraints on autoxidation and dimer formation from direct probing of monoterpene-derived peroxy radical chemistry, Proc. Natl. Acad. Sci. U. S. A., 115(48), 12142–12147, doi:10.1073/pnas.1812147115, 2018.